RSC Advances

ROYAL SOCIETY OF CHEMISTRY

www.rsc.org/advances

Graphical Abstract

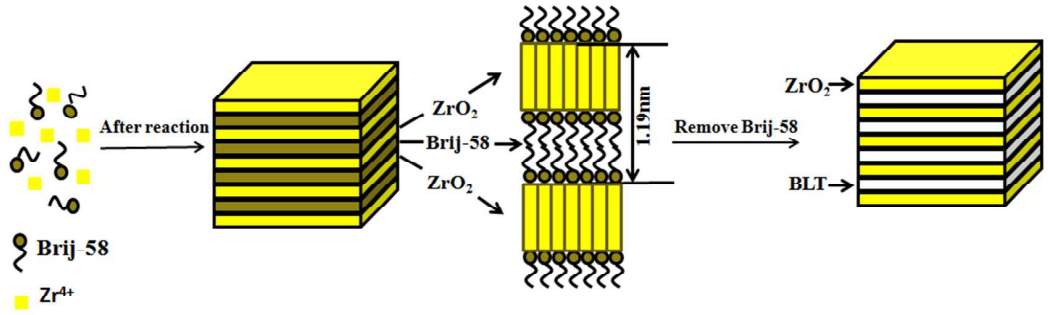

Lamellar formation mechanism of TSLCZ synthesized via Brij-58 template, The possible interaction between zirconia and Brij-58 was illustrated in Fig 6. Brij-58's hydrophilic head interacts with ZrO^{2+} and hydrophobic alkyl chain segments prefers to be close to each other via the hydrophobic interaction to form a bilayer template (BLT). With the crystal growth and the template guide, the 1.19 nm of period ordered lamellar superstructured crystalline zirconia were generated.

Brij-58 template synthesis of self-assembly thermostable lamellar crystalline zirconia via a reflux-hydrothermal hybrid method

Penghe Su,[1] Xiujie Ji,[1,*] Chao Liu,[2] Wenjun Gao,[1] Ranran Fu,[1] Chengchun Tang,[2] Bowen Cheng[1]

[1]State Key Laboratory of Hollow Fiber Membrane Materials and Processes, Tianjin Polytechnic University, Tianjin 300160, China

[2]School of Materials Science and Engineering, Hebei University of Technology, Tianjin 300130, China

* X.J. Ji

Corresponding ,author. Tel: +86 022 83955800.

E-mail address: JXJ_TJPU@163.com (Xiujie Ji).

Abstract

By using polyoxyethylene-20-cetyl-ether (Brij-58) as supramolecular template, the thermostable lamellar crystalline zirconia (TSLCZ) was synthesized though the reflux-hydrothermal hybrid method (R-HT) with $ZrOCl_2 \cdot 8H_2O$ as zirconium source, sodium hydroxide as precipitating agent. The TSLCZs were characterized by XRD, TEM, SAED, FE-SEM, TG-DTA and FTIR. X-ray diffraction (XRD) and Fourier transform infrared spectroscopy (FTIR) analyses showed that zirconia is the only crystal phase in TSLCZ and Brij-58 promoted zirconia nucleation and 2D-growth, and induced self-ordered lamellar nanostructured assembly. Transmission electron microscope (TEM) observation further proved this regular lamellar structure detected by XRD. The repeat periodicity of the structure is about 1.20 nm observed by TEM, which is in well accordance with the XRD data (1.19 nm). The selected area electron diffraction (SAED) results indicated that TSLCZ was a polycrystalline structure. XRD, TEM and Field Emission Scanning Electron Microscopy (FE-SEM) results show that, the TSLCZ can be well preserved even after high temperature thermal treatment at 500 °C for 2 h. Moreover, R-HT significantly promoted Brij-58 directed synthesis of TSLCZ in three aspects of heterogeneous nucleation, controlled 2-D growth and ordered lamellar self-assembly than only reflux (R) or hydrothermal (HT) method. The possible formation of the TSLCZ could be explained by a surfactant template.

Keywords: Zirconia, Brij-58, Nanocrystalline materials, Self-assembly, Lamellar

1. Introduction

Self-assembly is the spontaneous association of an ensemble of molecules into one or more supramolecular. Self-assembly allows for the construction of complex, adaptable, and highly tunable materials. The use of self-assembly for the construction of functional materials now is a highly promising and exciting area of research. Over the past ten decades, a number of self-assembly materials have been successfully synthesized, such as functional biomaterials [1], “ tree-like ” amphiphilic glycopolypeptidesw [2], complex hollow materials [3], triphenylene-containing conjugated macrocycles [4], N-isopropylacrylamide [5], branched glycopolypeptides [6], TiO_2 nanoparticles [7], Zirconium Titanate [26], and so on.

Zirconia is one of the most important functional metal oxides materials, which can be widely used as catalysts and catalyst supports [8-10], dielectric materials [11], ceramic [12], solitary photocatalytic materials [13-14], solid oxide fuel cells [15] and so on. Recently, self-assembled highly crystalline thermally stable zirconias have been considered as an important material due to several unique properties[16, 20]. A series of self-assemble ordered superstructured zirconia materials have been successfully synthesized through surfactants ,such as anionic surfactant [17-19], blockcopolymer [20], cationic surfactant [21] and composite surfactant [22]. Unfortunately, in most cases, the ordered superstructured zirconia synthesized is still far from satisfactory, the crystalline framework and the corresponding superstructure will collapsed during the subsequent crystallization or heat treatment, which remains synthesis of thermostable self-assemble ordered lamellar superstructured crystalline

zirconia a great challenge that severely hinders the practical applications.

Brij-58($C_{16}H_{33}O(CH_2CH_2O)_{20}H$) is a common nonionic surfactant which has a calculated HLB value of 15.7. This surfactant was used in solubilizing proteins [23], porous hydrogel [24], nanoporous carbons [25], mesoporous zirconium titanium oxide thin films [26] and so on, but there is no reports have been found about Brij-58 assisted synthesis of ordered lamellar materials.

Herein the Brij-58 template was successfully applied to synthesize thermostable lamellar crystalline zirconia (TSLCZ). The possible synthesis mechanism via this novel Brij-58 template is discussed.

2. Experimental

(1) Materials

$ZrOCl_2•8H_2O$, NaOH were all analytical grade reagents Sinopharm Chemical Reagent Co., Ltd. (Shanghai, China), deionized water was also used in the experiment. Nonionic surfactant polyoxyethylene 20 cetyl ether (Brij-58, M_w=1123.5, SERVA Company), HLB (hydrophile-lipophile balance)=15.7, was of analytic grade and was used as received without further purification.

(2) Synthesis of TSLCZ via R-HT route

A typical synthesis process as follows: 0.72 g of NaOH and 0.75 g Brij-58 were dissolved in 50 mL water. Under vigorous stirring, it was slowly added to 50 mL solution of 0.97g $ZrOCl_2•8H_2O$. After refluxed for 2 h under stirring, the resulting

suspension was sealed in a PTFE-lined stainless steel autoclave and crystallized at 160℃ for 12 h. After cooled and deposited at room temperature for 12 h, the precipitate was filtered and dried at 60℃. The white thermostable lamellar crystalline zirconia (TSLCZ) powder was gained. The as-synthesized TSLCZ was calcined in air from roomtemperature to 500℃ at a heating rate of 5℃/min, and maintained at 500℃ for 2h, then cooled to roomtemperature. The calcined TSLCZ was obtained. The samples are prepared in R-HT, R, HT methods were shown in Table 1.

(3) Characterization

The samples are prepared in reflux (R), reflux-hydrothermal hybrid method (R-HT), hydrothermal (HT) and calcined methods were analyzed and compared by powder X-ray diffraction (XRD), transmission electron microscopy (TEM) and Field Emission Scanning Electron Microscopy (FE-SEM). XRD data were recorded by Rigaku D/max 2500PC X-ray diffractometer (Rigaku Corporation, Tokyo, Japan), Cu Ka target, voltage of 40 kV, current of 150 mA, scan range 3–80° and step 0.02°. TEM date was observed by JEM-2100 [JEOL Ltd., Tokyo, Japan], 100 kV. FE-SEM date were observed on a field emission scanning electron microscopy (FE-SEM, Hitachi S-4800) at 10.0 kV after sputter coated with gold under vacuum. The thermostable lamellar crystalline zirconia (TSLCZ) was characterized by Fourier transform infrared spectroscope (FT-IR) and Thermal gravimetry and differential thermal analysis (TG-DTA). Fourier transform infrared spectroscope

(FTIR,TENSOR37, German) spectra were recorded over the range from 400 to 4000 cm^{-1} after mixed with KBr powder. TG-DTA studies were carried out between room temperature and 1300 °C on a Seiko TG/DTA 6300.

3. Results and Discussion

(1) X-Ray Diffraction (XRD) Analysis

In order to investigate the Brij-58 template roles on the ordered lamellar superstructure and crystallization, (b) Calcined, (c) HT, (d) R were synthesized for comparison.

The samples were analyzed by XRD (Fig. 1.). As shown in the small angle XRD (SAXRD, 2θ = 5-10 °) of the four samples synthesized via different routes, significant peaks were detected at 2θ =7.38° and 8.72° [labelled by L(100)] {Figs. 1.(a) and (b)}. This SAXRD peak can be attributed to ordered lamellar nanostructure. According to Bragg equation (Eq. (A.1)),

$$2d \sin\theta = n\lambda \qquad (1)$$

where λ = 0.15406 nm, corresponding calculated repeat period were 1.19 nm.

According to the lamellar formula (Eq. (A.2)) [29,30]:

$$d_{hkl} = a / (h^2 + k^2 + l^2)^{1/2} \qquad (2)$$

where a is the lamellar parameter, a_1 = 1.19 nm {Fig. 1.(a)} and a_2 = 1.01 nm {Fig. 1.(b)}. Through the above calculation, reflects that the corresponding lamellar period justs lightly shrank from 1.19 to 1.01nm during the calcination at 500℃(confirmed by Figs. 2.(a) and (b)), and the ordered lamellar superstructure is well thermostable.

Furthermore, comparing the SAXRD peaks of R, HT and R-HT, R-HT have the most obvious (100) diffraction peak. This indicated that R-HT method significantly

promoted the Brij-58 templating role on the ordered superstructure.

The WAXRD (2θ = 10-70 °) R, HT and R-HT shown that HT and R-HT method can promoted the crystallization, as a result a mixed phase of monoclinic and cubic was obtained, and the latter are the main phase. Samples are mixed with an ordered lamellar crystalline zirconium oxide nanostructure, thus seen from the different preparation methods only affect the phase composition ratio of the product, and the apparent degree of crystallinity of the product. In addition, the difference of WAXRD patterns indicated R-HT not only effectively induced the self-assemble of the TSLCZ, but also significantly controlled the zirconia nucleation and crystal growth.

In summary, R-HT are the best candidate for Brij-58 templating synthesis of the thermostable lamellar crystalline zirconia.

(2) Transmission Electron Microscopy (TEM) Observation

For further support of the XRD analysis, TEM was used to observe the morphologies of the samples synthesized via different routes. (Fig. 2.). As shown in Figs. 2. (a) and (b), it can be seen that a 1.20 nm and a 1.00nm of period structures, and the dark and light thickness is of about 0.6 nm and 0.5 nm, alternately. Because XRD (Fig. 1.) and FTIR (Fig. 5.) analyses have shown no other crystal phases, except for pure zirconia, this ordered nano-array should consists of zirconia layer (dark) and pore layer (light), alternately. These dates are well agree with the 1.19 nm and 1.01 nm of calculated results from SAXRD (confirmed by Figs. 1.(a) and (b)). Fig. 2.(b) shows the

corresponding selected area electron diffraction (SAED) pattern taken from ordered nanoarray of TSLCZ after been calcination. The SAED results indicate that the TSLCZ is polycrystalline. The rings are sharp and continuous, which shows that the TSLCZ is highly crystalline. TEM and SAED analysis further support that of the ordered lamellar structure of TSLCZ exhibits good thermostability at 500 °C.

In contrast, there were no ordered lamellar structures were found in the samples synthesized by only R and HT methods.

(3) Field Emission Scanning Electron Microscopy (FE-SEM) observation

The samples synthesized though these different methods were observed by FE-SEM. Figs. 3.(a) and (b) show that the morphologies of the as-synthesized and calcined TSLCZ have no significant changes, which show similar multilayers morphologies (confirmed by Figs .1.(a) and (b) and .2.(a) and (b)). This reflects that TSLCZ is of very good morphology thermostability at 500 °C. In contrast, the products synthesized via R and HT route exhibit different morphologies (as shown in Figs. 3.(c) and (d)), specifically, none of them are exhibiting the multilayers morphology. The difference between them is that the latter (Fig. 3(d)) shows a much more clear shape and boundary than the former (Fig. 3(c)). This reflects the different crystallinities of them as presented in (Figs. 1(c) and (d)).

(4) Thermal gravimetry and differential thermal analysis (TG-DTA) analysis of TSLCZ

TG-DTA was used to observe the morphologies of the samples, TG-DTA results of TSLCZ is shown in (Fig. 4.). For the case of TSLCZ, there was one period of weight loss. The period occurred at 0 °C to 200 °C, due to the loss of physically adsorbed water. And then, the weight almost has little change form 200 °C to 1200 °C. On the other hand, in the whole process, there was no obvious endothermal and exothermic peaks in the DTA Curve which indicated that the TSLCZ synthesized though R-HT the method with high stability.

(5) Fourier transform infrared spectroscope (FTIR) analysis of TSLCZ

In order to examine the samples prepared by these different methods whether containing the template Brij-58, The FTIR spectra of Brij-58 and the samples prepared by these different methods were analyzed by FTIR (Fig. 5.). As can be seen from Figs. 5. (a), (b) and (d) : the absorption peak appearing at 3431 cm^{-1} should be assigned to the stretching vibration of the sample water-binding group H-O; The absorption bands occur at 1638 cm^{-1} and 1352 cm^{-1} were the bending vibration peaks, belonging to the Coordinated water and the Coordination hydroxyl group, respectively; The corresponding absorption peaks of Zr-O (970, 758 and 586cm^{-1} in Figs. 5. (a), (b) and (d)) were also to be found in the samples. For Brij-58 (Fig. 5. (c)), a triple peak appears at 1062-1146 cm^{-1}, which could be attributed to the $-CH_2-O-CH_2-$ stretching vibration. In comparison with Figs. 5. (a), (b), and (d), no clear triple peak of Brij-58 were founded in the absorption peaks, whereby the

description, the Brij-58 acts as the template nanostructure in the preparation of ordered crystalline layered zirconium oxide, and has been get rid off during the hot water washing and drying process. But, only the R-HT method can synthesize the self-assembly thermostable lamellar crystalline zirconia without post-treatments.

(6) Template Action of Brij-58 in TSLCZ

From these experiments, Brij-58 template role and synthesis mechanism of TSLCZ (Fig. 6.) may be described as follows: Brij-58 containing hydrophilic polyoxyethylene and hydrophobic alkyl chain segments will associate each other through hydrophobic interaction and electrostatic force to minimize the system free energy. Thus Brij-58 would form spherical, cylindrical and layered structure under various concentrations on account of differences upon surface tension. Brij-58's hydrophilic head interacts with ZrO^{2+} and hydrophobic alkyl chain segments prefers to be close to each other via the hydrophobic interaction to form a bilayer template (BLT). In this nanohybrid system, the Brij-58 selectively adsorbs on the amorphous zirconia surface, as a result the interface energy (σ) of the nucleus decreases. Moreover, amorphous zirconia has higher supersaturation (S) in this micro-phase-separated nanohybrid system than in the solution phase.

According to the Gibbs free energy equation of nucleation [27-30] ,

$$\Delta G^* = B\sigma^3 V^2/(kTlnS)^2$$

Wherein, ΔG * refers to the critical free energy, B is a constant, σ is the interfacial energy, V is the volume of the molecule, k is the Boltzmann constant, T is the absolute temperature, S is the supersaturation.

The two parameters (σ and S) cause the critical nucleation free energy (ΔG *) decrease. Accordingly, the crystal nuclei are much easier to form in this micro-phase-separated nano hybrid system. With the crystal growth and the template guide, the 1.20 nm of period ordered lamellar superstructured crystalline zirconia were generated via the Brij-58 supramolecular template.

Therefore, nuclei can be formed in priority in this micro-phase separated hybrid, and zirconia crystallized in situ under the control of Brij-58 template, and then grow into layered particles between the bilayer Brij-58 template.

4. Summary

In this article, we successfully used Brij-58 as independent soft template to synthesize the self-assembly thermostable lamellar crystalline zirconia without post-treatments. Brij-58 played a role of the template in the preparation of ordered crystalline layered nanostructures zirconia, on the one hand promoted zirconia nucleation and growth; other hand, induces a self-assembly layered nanostructures assembly. Moreover, R-HT route well promoted Brij-58 supermolecular template role and may be useful for the syntheses of other selfassembly nanostructured materials with good thermostabilities. The possible mechanism may be described by a novel Brij-58 templating synthesis.

5. REFERENCES Acknowledgments

This study is supported by National Natural Science Foundation of China (50902043 and 21104057) , Natural Science Foundation of Hebei Province (E2009000081and E2015202069). We greatly appreciate the reviewers' valuable comments.

6. References

[1] N. Stephanopoulos, J. H. Ortony, and S. I. Stupp, Acta Metall., 2013, 61912-61930.

[2] C. Bonduelle, J. Huang, E. Ibarboure, A. Heisec and S. Lecommandoux, Chem. Commun., 2012, 48, 8353- 8355.

[3] H. C. Zeng, J. Mater. Chem., 2011, 21, 7511.

[4] T. Dutta, Y. Che, H. Z. Zhong, J. H. Laity, V. Dusevich, J. B. Murowchick, L. Zang and Z. H. Peng. RSC Adv., 2013, 3, 6008.

[5] Y. L. Yi and S. X. Zheng. RSC Adv., 2014, 4, 28439.

[6] C. Bonduelle, S. Mazzaferro, J. Huang, O. Lambert, A. Heise and S. Lecommandoux, Faraday Discuss., 2013, 166, 137.

[7] S. K. Das, M. K. Bhunia and A. Bhaumik., Dalton Trans., 2010,39, 4382- 4390.

[8] M. Labaki, H. Laversin, E. A. Zhilinskaya, A. Aboukaïs, and D. Courcot, Catal. Commun., 2012, 17, 64- 70.

[9] M. Signoretto, F. Menegazzo, L. Contessotto, F. Pinna, M. Manzoli, and F. Boccuzzi, Appl. Catal. B: Environ., 2013, 129, 287- 293.

[10] X. H. Zhang, H. Q. Su, and X. Z. Yang, J. of Mol. Catal. A: Chem. , 2012, 360, 16- 25.

[11] O. Bethge, C. Henkel, S. Abermann, G. Pozzovivo, M. Stoeger-Pollach, W. S. M. Werner, J. Smoliner, and E. Bertagnolli, Appl. Surf. Sci., 2012, 258, 3444- 3449.

[12] D. HANAOKA, R. IT, and Y. FUKUZAW, J. Adv. Mech. Des. Sys., 2011, 5, 372- 384.

[13] A. A. Ashkarran , S. A. A. Afshar, S. M. Aghigh, and M. kavianipour, Polyhedron, 2010, 29, 1370- 1374.

[14] T. Sreethawong, S. Ngamsinlapasathian, and S. Yoshikawa, Chem. Eng. J. , 2013, 228, 256- 262.

[15] H. J. Cho, and G. M. Choi, J. Power Sources, 2008, 176, 96- 101.

[16] D. H. Deng, X. P. Liao, X. Liu, and B. Shi, J. Mater. Res., 2008, 23, 3263-3268.

[17] E. Zhao, O. Hernández, G. Pacheco, S. Hardcastle, S. Hardcastle and J. J. Fripiat, J. Mater. Chem., 1998, 8(7), 1635- 1640.

[18] G. Pacheco, E. Zhao, A. Garcia, A. Sklyarov and J. J. Fripiat, Chem. Commun., 1997, 491- 492.

[19] G. Pacheco, E. Zhao, A. Garcia, A. Sklyarov and J. J. Fripiat, J. Mater. Chem. 1998, 8(1), 219- 226.

[20] S. K. Das, M. K. Bhunia, A. K. Sinha, and A. Bhaumik, J. Phys. Chem. C, 2009, 113, 8918- 8923.

[21] U. Ciesla, M. Fröba, G. Stucky, and F. Schüth, Chem. Mater., 1999, 11, 227-234.

[22] H. R. Chen, J. L. Gu, J. L. Shi , Z. C. Liu, J. H. Gao, M. L. Ruan, and D. S. Yan, Adv. Mater. , 2005, 17, 2010- 2014.

[23] L. Isaksson , J. Enberg , R. Neutze, B. Göran Karlsson and A. Pedersen, Protein Expres. Purif., 2012, 82, 218- 225.

[24] W. J. Gao, Q. S. Zhang, P. F. Liu, S. H. Zhang ,J. Zhang and L. Chen, RSC Adv., 2014, 4, 34460- 34469.

[25] J. Choma , A. Żubrowska , J. Górka, and M. Jaroniec, Adsorption, 2010, 16, 377-383.

[26] V. Luca, E. Drabarek, C. S. Griffith, and T. L. Hanley, Chem. Mater. , 2010, 22, 3832- 3842.

[27] C. Liu ,S. S. Zhao, X. J. Ji, B. Wang, and D. X. Ma, Mater. Chem. Phys., 2012, 133, 579- 583.

[28] X. J. Ji , C. Y. Liu , C. Liu, J. Li, X. F. Yu, P. H. Su, J. R. Huang, J. L. Jia, J. Wu, L. Y. Chen, C. H. Chen, Y. J. Wu, Y. Fan, J. Lin, B. W. Cheng, and C. C. Tang, Mater. Lett., 2014, 122, 309- 311.

[29] C. Liu, X. J. Ji, and G. X. Cheng, Appl. Surf. Sci., 2007, 253, 6840- 6843.

[30] C. Liu, D. X. Ma, X. J. Ji, S. S. Zhao, S. Li, Appl. Surf. Sci., 2011, 257, 4529-4531.

Caption of Figures

Fig. 1. XRD patterns of (a) R-HT, (b) Calcined, (c) HT, (d) R methods, L ordered lamellar superstructure, M monoclinic ZrO_2, and C cubic ZrO_2.

Fig. 2. TEM images of (a) R-HT, (b) Calcined, (c) R, (d) HT methods via Brij-58 template. SAED image of calcined TSLCZ was inserted in Fig.2.(b).

Fig. 3. FE-SEM images of (a) R-HT, (b) Calcined, (c) R, (d) HT methods via Brij-58 template.

Fig. 4. TG-DTA image of TSLCZ via Brij-58 template.

Fig. 5. FTIR spectrum of (a) HT, (b) R, (c) Brij-58, (d) R-HT.

Fig. 6. Lamellar formation mechanism of TSLCZ synthesized via Brij-58 template, the possible interaction between zirconia and Brij-58 was illustrated in Fig 6.

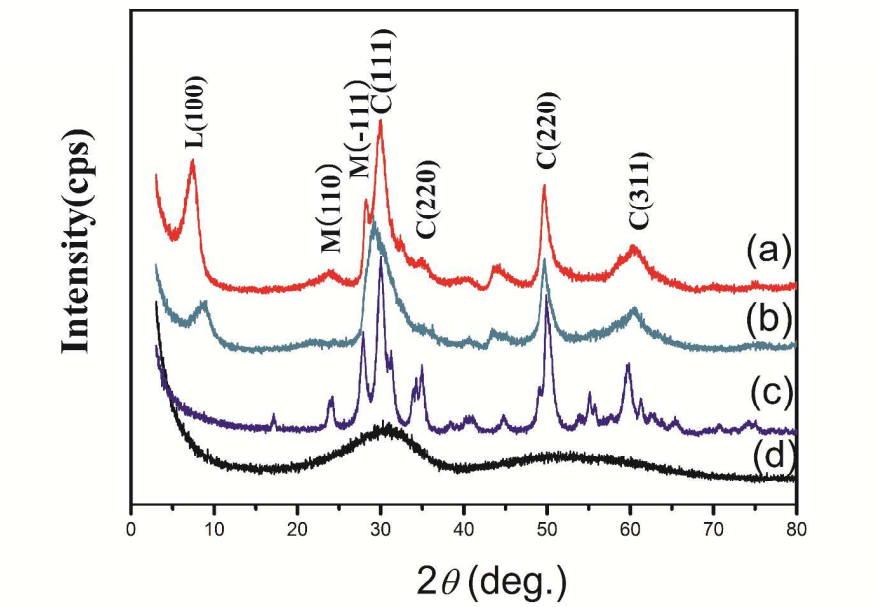

Fig. 1. XRD patterns of (a) R-HT, (b) Calcined, (c) HT, (d) R methods, L ordered lamellar superstructure, M monoclinic ZrO_2 and C cubic ZrO_2.

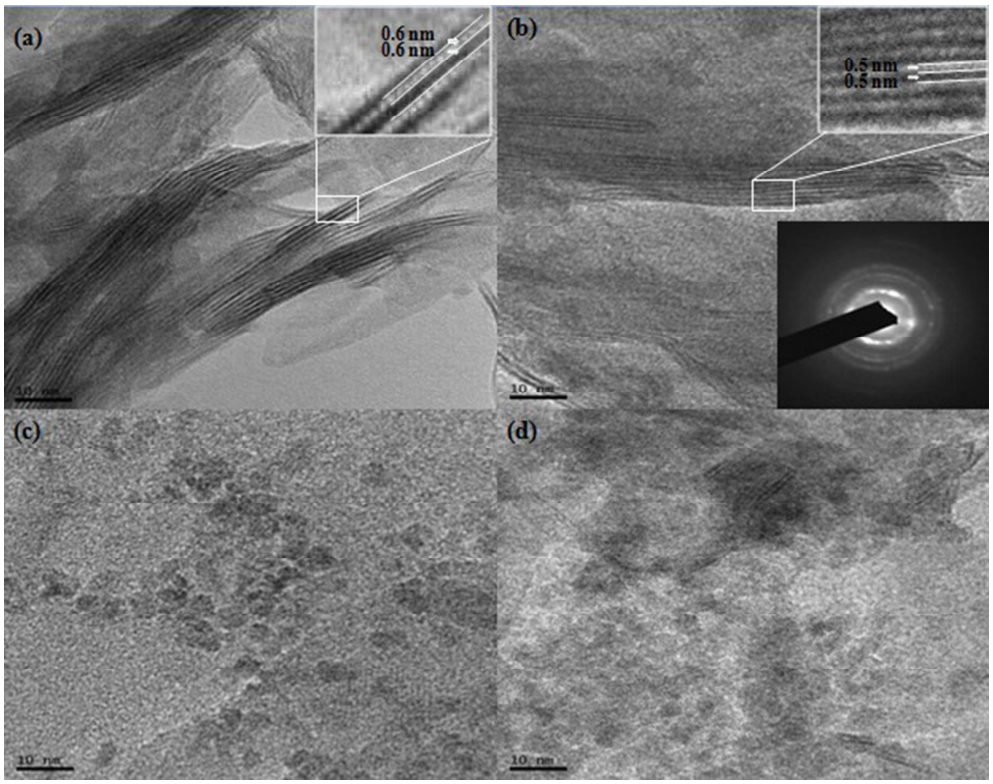

Fig. 2. TEM image of (a) R-HT, (b) Calcined, (c) R, (d) HT methods via Brij-58 template. SAED image of calcined TSLCZ in Fig.2.(b).

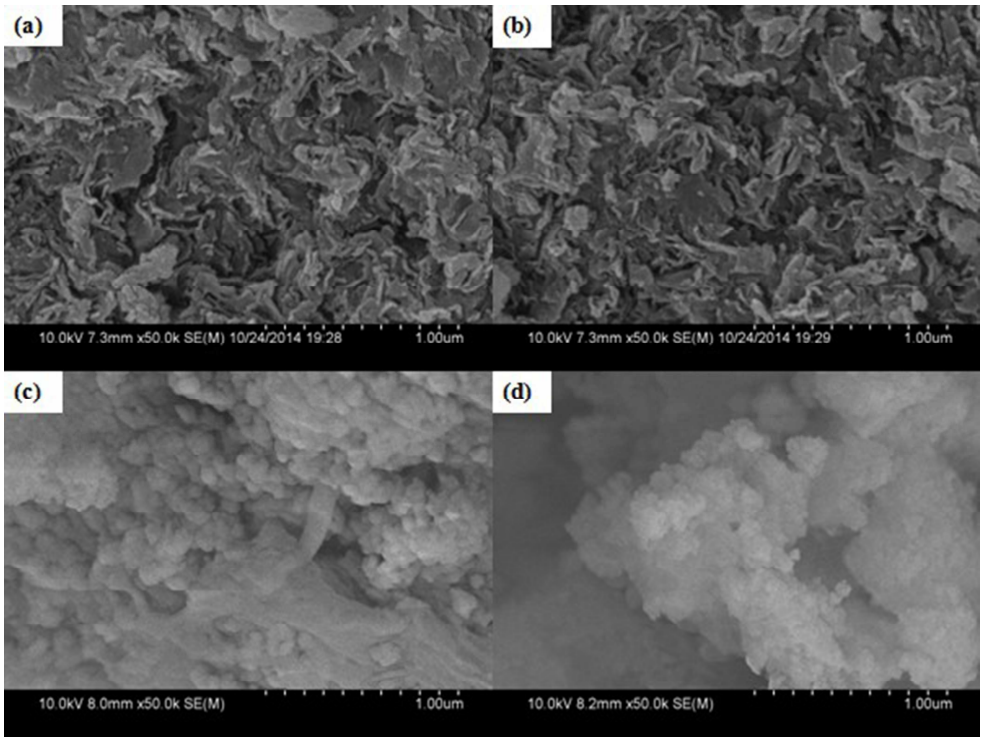

Fig. 3. FE-SEM images of (a) R-HT, (b) Calcined, (c) R, (d) HT methods via Brij-58 template.

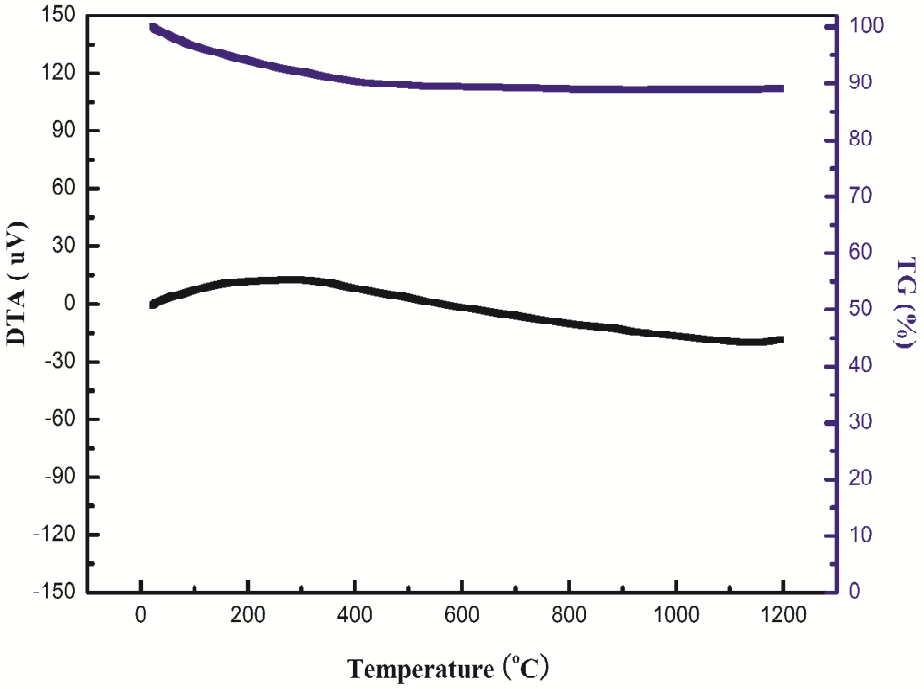

Fig. 4. TG-DTA image of TSLCZ via Brij-58 template.

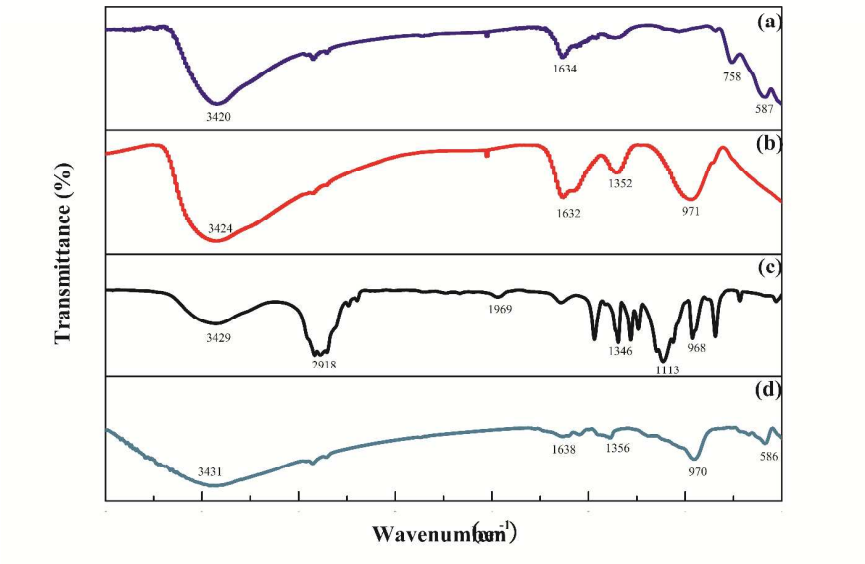

Fig. 5. FTIR spectrum of (a) HT, (b) R, (c) Brij-58, (d) R-HT.

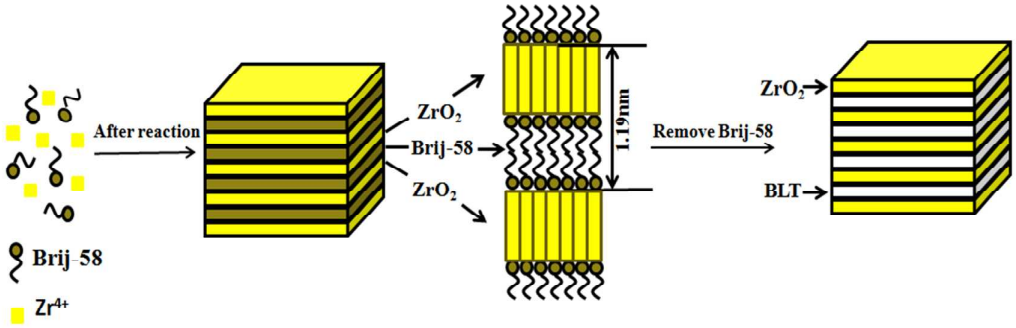

Fig. 6. Lamellar formation mechanism of TSLCZ synthesized via Brij-58 template,

The possible interaction between zirconia and Brij-58 was illustrated in Fig. 6.

Table 1

Synthesis recipes of different methods.

Method	$ZrOCl_2$	NaOH	Brij58	Refux time at 100℃	Hydrothermal time at 160℃
R-HT	0.003mol	0.018mol	0.75g	2h	12h
R	0.003mol	0.018mol	0.75g	2h	-
HT	0.003mol	0.018mol	0.75g	-	12h